Available online at www.sciencedirect.com

SciVerse ScienceDirect

Ceramics International 38 (2012) 6099–6105

CERAMICS INTERNATIONAL

www.elsevier.com/locate/ceramint

Microwave-hydrothermal synthesis of extremely high specific surface area anatase for decomposing NO_x

Sonthikan Sitthisang[a,b], Sridhar Komarneni[a,*], Jonggol Tantirungrotechai[b], Young Dong Noh[a], Huihui Li[c], Shu Yin[c], Tsugio Sato[c], Hiroaki Katsuki[d]

[a] *Materials Research Institute, Materials Research Laboratory, The Pennsylvania State University, University Park, PA 16802, USA*
[b] *Department of Chemistry, Faculty of Science, Mahidol University, Rama 6 Road, Bangkok 10400, Thailand*
[c] *Institute of Multidisciplinary Research for Advanced Materials, Tohoku University, Sendai 980-8577, Japan*
[d] *Saga Ceramics Research Laboratory, 3037-7, Arita-machi, Saga, 844-0022, Japan*

Received 15 February 2012; received in revised form 5 April 2012; accepted 21 April 2012
Available online 4 May 2012

Abstract

Apparently C-doped and undoped or pure nanoparticles of anatase were synthesized using a microwave hydrothermal process in the temperature range of 140–180 °C for 1 h from several Ti precursors, such as Ti ethoxide, Ti isopropoxide and Ti oxysulfate. Nanoparticles of anatase samples were characterized by powder X-ray diffraction, transmission electron microscopy (TEM) and photocatalytic activity measurements. Results showed that nanoparticles in the size range of 4–17 nm of anatase were obtained in all cases with surface areas in the range of 151–267 m^2/g. The photocatalytic activity of the prepared titanias was measured using methylene blue (MB) and NO_x molecules. Because MB has very strong adsorption on the samples, photocatalytic degradation under either solar light or black light irradiation was found to be very limited. However, the $DeNO_x$ abilities of carbon-doped titanias were higher than those of Degussa P25 commercial titania sample and undoped or pure titanias especially under irradiation by long wavelength or visible light (> 500 nm).

Keywords: Carbon-doped anatase; Microwave-hydrothermal synthesis; $DeNO_x$ ability; Photocatalytic activity

1. Introduction

Titania or titanium dioxide is a naturally recurring mineral, and it is well-known that it has three polymorphs, i.e., anatase, rutile and brookite. The formation of a particular polymorph depends on starting material, synthesis method, calcination temperature, etc. Titania has a lot of applications, such as pigment, sunscreen, semiconductor and photocatalyst, because it is cost-effective, non-toxic and stable. It is widely used as a white pigment because of its brightness and very high refractive index. In cosmetic and skin care products, it was used for sunscreen because of its protection from UV radiation. Since the early 1970s' titanium dioxide, TiO_2 has been developed as a semiconductor photocatalyst that can be used for solar energy conversion, water splitting, water and air purification and self-cleaning application of surfaces [1,2].

Fujishima and Honda [1] found that water can be decomposed into oxygen and hydrogen on TiO_2 electrode by irradiating light of wavelength shorter than 415 nm irradiation. This work has triggered research on synthesis of titania by many methods. There are various methods for synthesis of TiO_2, such as sol–gel, solid-state, chemical vapor deposition, hydrothermal process, etc. The solid-state synthesis process is the most commonly used technique for ceramic material's synthesis, while sol–gel has become popular in the last several decades. The sol–gel process starts from inorganic metal salts or metal organic compounds, which will form network structures by carefully controlled hydrolysis and polymerization reactions [3–5]. Chemical vapor deposition (CVD) is the process in which a vapor state of a material is condensed to form a solid-phase material. This process is often used in the semiconductor

---

*Corresponding author.
E-mail address: komarneni@psu.edu (S. Komarneni).

0272-8842/$36.00 © 2012 Elsevier Ltd and Techna Group S.r.l. All rights reserved.
http://dx.doi.org/10.1016/j.ceramint.2012.04.057

industry to produce thin films, and therefore, CVD is a good method for coating TiO_2 onto many particles, such as silica gel, fumed silica, ZSM-5, etc. [6–9]. For example, Wu et al. have developed a method to synthesize carbon-doped TiO_2 spheres on Ti substrates and carbon-doped TiO_2 nanotubes within nanochannels of alumina template by using CVD process [10].

Hydrothermal method has recently become one of the most widely used methods to obtain nanophases of ceramics although overall chemical routes performed under usual pressures are more widely used methods than hydrothermal ones. Conventionally, it is conducted in autoclaves with Teflon vessels under controlled high temperature and high vapor pressure. It is easy to adjust particle size, shape and crystallinity of metal oxides by changing reaction temperature, pH, additives, heating time, etc. Therefore, the hydrothermal method has become very popular for synthesis of TiO_2 [11]. One of the disadvantages of the conventional hydrothermal process is that it uses long heating time of several hours. For faster hydrothermal process, Lazau and coworkers developed a novel fast-hydrothermal method that reduced the synthesis-cycle time to 15–30 min (fast-hydrothermal) [12]. Another way to cut down synthesis-cycle time and energy usage is the use of microwave hydrothermal method. Microwave radiation was applied to prepare various metal oxides including TiO_2 by Komarneni and coworkers in 1992 and they coined the term "microwave-hydrothermal" process [13]. The microwave hydrothermal process used only 0.5–2 h for synthesis of rutile titania. On the other hand, conventional hydrothermal process needed more than 72 h for rutile phase using the same chemicals [13]. In later studies, they controlled particle size, morphology, and polymorph of titania under microwave-hydrothermal conditions by adjusting the various reaction parameters, such as pH, heating time, pressure, etc. [14]. Very recently, Yin et al., synthesized nitrogen-doped titania nanoparticles by the microwave hydrothermal method in 5–60 min and they showed excellent photocatalytic ability for the oxidative destruction of nitrogen monoxide under irradiation of both visible-light ($\lambda > 510$ nm) and UV light [15,16].

During the earlier years of photocatalyst development, unsubstituted or undoped TiO_2 was widely used in air or water purification. Because the band gap of TiO_2 is 3.2 eV, it requires the UV light for effective photocatalytic activity, but this is only 3–5% in solar light. Because visible light is the main part of solar light, increasing the photocatalytic degradation property of titanium dioxide in visible light is of paramount importance. To achieve this, many studies of doping TiO_2 with metals, such as Cu, Co, Ni, Cr, Mn, Mo, V, Fe, Au, Ag, etc. [17–28] or non- metals, such as N, S, C, B, P, I, F, etc.[11,12,16,22,29–37] were done to lower the band gap of titania. For metal-doped TiO_2, the photocatalytic activity in visible light can be explained by the fact that an electron is promoted to a new conduction band that has lower energy than with the undoped sample. On the other hand, for titania doped with nonmetals, there are three main hypotheses to explain the mechanism of TiO_2 for the photocatalytic activity in visible light, i.e., band gap narrowing, impurity energy levels, and oxygen vacancies [38–41]. The main non-metal dopants are carbon or nitrogen, but carbon-doped TiO_2 was shown to be more active for photocatalysis reaction than N-doped TiO_2 [42].

For the above reason, there are numerous experimental studies that report on the synthesis of carbon-doped TiO_2. For example, Li et al. successfully prepared carbon-doped titania by hydrothermal process, and the sample showed highly efficient photocatalytic activity, i.e., about 11 times higher than that of Degussa P25 TiO_2 in degradation of methyl orange [43]. Another example is by Lee et al. who synthesized carbon-doped titania with a mesoporous structure in a simple one-step chemical synthesis. This carbon-doped titania has high photocatalytic activity under visible light at a wavelength of less than 550 nm [44]. The final example is that by Dong et al., who developed a green synthetic route for visible light photocatalytic materials. This method produced pure product using minimum energy and without harmful reagents or unstable precursors. Glucose $(C_6H_{12}O_6)_{36}$ was commonly used as a green chemical precursor as the carbon dopant for TiO_2. The above carbon-doped TiO_2 had good photocatalytic activity for degradation of toluene in the gas phase under visible light irradiation compared to commercial grade Degussa P25 [33]. There is still a need to develop greener, faster and better carbon doped TiO_2 materials for photocatalytic activity in visible light.

Therefore, the objective of this study was to develop a simple one-step microwave-hydrothermal process for synthesis of carbon-doped TiO_2 for photocatalytic reactions. Microwave-hydrothermal process is a green process, which leads to considerable energy savings because of rapid synthesis [14,15,33,45].

2. Experimental section

2.1. Materials

The following chemicals were used for synthesis of titania under different conditions: titanium (IV)isopropoxide, $C_{12}H_{28}O_4Ti$ (98% Acros Organic), titanium (IV) oxysulfate sulfuric acid, $TiOSO_4 \cdot xH_2O + H_2SO_4$ (81.7% Alfa Aesar), titanium (IV) ethoxide (99% Alfa Aesar), D-(+)-glucose, $C_6H_{12}O_6$ (99.5% Sigma Aldrich), D-(+)-sucrose, $C_{12}H_{22}O_{11}$ (99.5% Fluka) and β-cyclodextrin, $C_{42}H_{70}O_{35}$ (Alfa Aesar). All the titania samples were synthesized using the above chemicals in de-ionized (DI) water.

2.2. Methods

2.2.1. Microwave hydrothermal synthesis

First, 0.0125 mol of titanium precursor were mixed with a carbon source (glucose, sucrose or cyclodextrin) and 35 ml of DI water by stirring in a Teflon vessel. The molar ratios of glucose, sucrose, and cyclodextrin to titanium precursors are 1:50, 1:100 and 1:350, respectively. Then, the Teflon vessel was hydrothermally heated at different temperatures of 140 °C, 160 °C or 180 °C for 1 or 2 h by the microwaves in a MARS-5 instrument. This M-H system operates under controlled temperature or pressure conditions using a 2.45 GHz frequency. The power of this unit can also be controlled from 0 to 100% with a total power of 1.2 KW, but all our experiments were conducted at a power of 300 W. The synthesized titania was separated by centrifugation and washed with DI water and ethanol several times to remove soluble species followed by drying in an oven at 60 °C. Undoped-TiO_2 samples were labeled as TI for samples made from titanium isopoproxide, TO for titanium oxysulfate-sulfuric acid and TE for titanium ethoxide. For carbon doped samples, they were designated as G-, S-, and D- for carbon sources of glucose, sucrose and cyclodextrin, respectively.

2.2.2. Characterization

All dried powder samples were characterized by powder X-ray diffraction (XRD) with Cu Kα radiation (40 kV, 40 mA) using an X' Pert MDP, PAN analytical instrument. This scan speed was $0.1358\ 2\theta\ s^{-1}$ to determine the crystal phases and their crystallite sizes. Morphology and particle sizes were observed by transmission electron microscopy (TEM). Titania powders were dispersed in alcohol, dropped onto copper grids that were coated with collodian and carbon films and then dried in air. The TEM images were obtained from JEM-2010 instrument (JEOL, Tokyo, Japan) at an acceleration voltage of 200 KV. The Brunauer-Emmett-Teller (BET) specific surface areas (S_{BET}) of the samples were analyzed by Autosorb-1 instrument made by Quanta Chrome Company. The BET surface areas were obtained at liquid nitrogen temperature using several values (Multi-point) of nitrogen adsorption in the P/P_0 range of 0.05–0.25. All the samples were degassed at 150 °C for 3 h prior to surface area measurements.

2.3. Photocatalytic activities

2.3.1. NO_x destruction

The photocatalytic activity for nitrogen monoxide destruction was determined by measuring the concentration of NO gas at the outlet of the reactor (373 cm^3 of internal volume) during the photo-irradiation of a constant flow (200 $cm^3\ min^{-1}$) of a mixture containing 1 ppm NO-50 vol.% air (balance N_2). The photocatalyst was placed in a hollow tube of 20 mm length × 16 mm width × 0.5 mm depth of a glass holder plate and set in the bottle at the center of the reactor. The photocatalyst under test was first equilibrated with the flowing NO gas before turning on the light. A 450 W high-pressure mercury arc was used as the light source. The wavelength was controlled by selecting filters, i.e., Pyrex glass for >290 nm, Kenko L41 Super Pro (W) filter for >400 nm and Fuji triacetyl cellulose filter for >510 nm. The concentration of NO was determined using a NO_x analyzer (Yanaco, ECL-88A). It has been reported that during the photocatalytic destruction, about 20% of NO is directly reduced to N_2, and the other 80% is oxidized to NO_3^- species. For comparison, the photocatalytic reaction was also carried out using the standard commercial titania, Degussa P25.

2.3.2. Methylene blue (MB) decomposition

First, adsorption of methylene blue on titania without irradiation was determined. Photocatalytic degradation of MB was determined under different irradiation sources after adsorption-desorption equilibrium. The equilibrium concentration of MB was used as the initial value for the photodecomposition processes. MB degradation was conducted using a solar simulator as a light source (light intensity 70 W/m^2) and using an 8 W black light irradiation. MB decomposition experiments were conducted using 200 mg catalyst, 50 ml aqueous MB solution (initial concentration: 100 mg/L) under either solar light or black light irradiation.

3. Results and discussion

Table 1 shows the results of one undoped titania using Ti isopropoxide at 160 °C and several C-doped titania syntheses using titanium isopropoxide and ethoxide and various C sources, such as glucose, sucrose and cyclodextrin in the temperature range of 140–180 °C for 1 h. These samples are expected to be doped with carbon as previous results by Dong et al. [33] clearly showed C-doping of anatase in hydrothermally prepared titania with glucose at 160 °C. Carbon was proposed to be doped into the TiO_2 lattice in the form of substitutional carbon for oxygen sites as evidenced by XPS data [33]. Although we have not used XPS in this study to show carbon doping of anatase synthesized here, we are assuming that our samples prepared in a similar way are doped with C. Recently sophisticated analyses by Kremenovic et al., [46] of TiO_2 nanoparticles pointed out very complex nanostructure with amorphous skin that could help to retain the carbon as second phase. However, we could not detect any carbon phase although further studies would be needed to rule this out. All the syntheses yielded the single phase anatase as revealed by X-ray diffraction. We have verified that all samples are anatase using XRD data as no peak of brookite was present at 2.9A, XRD reflection (121) and no peak of rutile was present at 3.25A, XRD reflection (110). The XRD results revealed broad (101) reflections suggesting the formation of nanoparticles of anatase (Fig. 1). Crystal sizes of all the anatase samples were calculated based on Scherrer's formula using (101) reflection and are listed in Table 1. These results confirmed the formation of nanoparticles of anatase in the range of about 5–5.7 nm (Table 1). Transmission electron microscopy of selected samples further confirmed the formation of nanoparticles of anatase (Table 1 and Fig. 2). Selected anatase samples also showed very high specific surface areas, which are reflections of their nano-size (Table 1).

Table 1
Characteristics of C-doped titanias synthesized by microwave-hydrothermal reactions using Ti and C sources at different temperatures for 1 h.

Treatment				Characterization		
Ti source	C source	C:Ti	Temperature (°C)	Crystallite size (nm)		Specific surface area (m^2/g)
				XRD	TEM	
Ti ethoxide	Glucose	3:25[*]	140	5.2	–	–
Ti ethoxide	Glucose	3:25[*]	160	5.5	–	–
Ti isopropoxide	Glucose	3:25[#]	140	5.0	–	–
Ti isopropoxide	Glucose	3:25[#]	160	5.3	6–8	262
Ti isopropoxide	Glucose	3:25[#]	180	–	–	–
Ti isopropoxide	Glucose	9:25[¥]	140	5.1	–	–
Ti isopropoxide	Glucose	9:25[¥]	160	5.0	–	–
Ti isopropoxide	Glucose	9:25[¥]	180	5.2	–	–
Ti isopropoxide	Sucrose	3:25[#]	160	5.3	4–8	267
Ti isopropoxide	Sucrose	9:25[¥]	160	5.1	–	–
Ti isopropoxide	Dextrin	3:25[#]	160	5.7	–	236
Ti isopropoxide	None	–[Ψ]	160	5.6	5–10	235

[*] When C in Titanium(IV)ethoxide is included, the C: Ti ratio is 203: 25.

[#] When C in Titanium(IV)isopropoxide is included, the C: Ti ratio is 303: 25.

[¥] When C in Titanium(IV)isopropoxide is included, the C: Ti ratio is 309: 25.

[Ψ] When C in Titanium(IV)isopropoxide is included, the C: Ti ratio is 300: 25.

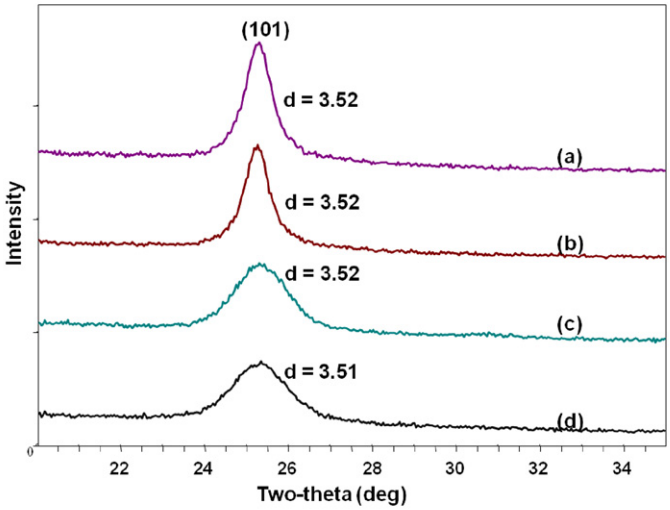

Fig. 1. XRD patterns of microwave-hydrothermally synthesized anatase at 160 °C/ 1 h, (a) from Ti oxysulfate, (b) from glucose+Ti oxysulfate, (c) Ti isopropoxide and (d) glucose+Ti isopropoxide.

Table 2 shows the results of hydrothermal syntheses of C-doped and undoped anatase, which were synthesized using titanium oxysulfate and various C sources at different temperatures for 1 h. Based on the XRD analyses, the crystal sizes of anatase formed from Ti oxysulfate with or without carbon source are larger than those from the Ti isopropoxide source (Tables 1 and 2; Fig. 1). The surface areas of anatase samples from Ti oxysulfate are also much smaller than those synthesized from Ti isopropoxide (Tables 1 and 2) again reflecting a larger crystal size with the former precursor. Transmission electron microscopy showed somewhat well-defined particles from pure Ti isopropoxide precursor, while those from pure Ti oxysulfate source showed slightly aggregated masses (Fig. 2a and b). However, the particles from all samples containing Ti oxysulfate showed larger particles than those samples containing Ti isopropoxide, confirming the results from XRD particle size analyses and surface area analyses (Tables 1 and 2).

Fig. 3 shows the XRD patterns of hydrothermally treated Ti oxysulfate and Ti isopropoxide with and without glucose as a carbon source at 160 °C for 1 h. All of them consisted of anatase phase. The carbon doped anatase samples exhibited almost exactly the same XRD patterns as those of undoped or pure anatase. Therefore, carbon doping did not significantly change the crystallinity or the polymorphic phase. The anatase phase derived from Ti isopoproxide showed broader (101) reflection than that from the Ti oxysulfate. The broadening of peaks is an indication of the smaller crystallite size and hence Ti isopoproxide yielded smaller crystals with higher surface area than the Ti oxysulfate precursor (Tables 1, 2 and 3). In general, the surface areas of carbon-doped TiO_2 were found to be slightly larger than those of the undoped-TiO_2 (Table 3).

The photocatalytic activity of the prepared titanias was measured using two model molecules, i.e., MB and NO_x. For an example, the MB adsorption and decomposition are shown for one anatase sample prepared from Ti isopropoxide with glucose at 160 °C for 1 h. MB has very strong adsorption on the anatase sample (Fig. 3a). Thus, photocatalytic degradation under either black light (Fig. 3b) or solar light irradiation (Fig. 3c) was limited. Therefore, we used NO_x decomposition to show the

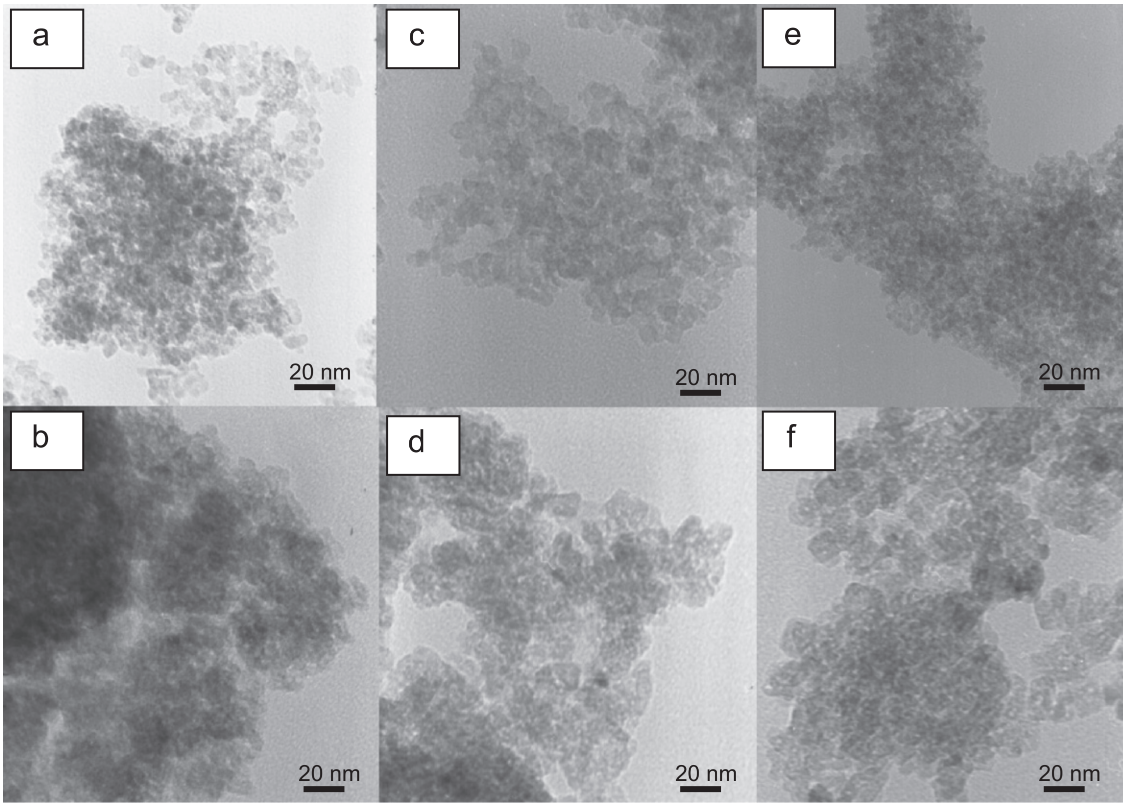

Fig. 2. TEM images of microwave-hydrothermally synthesized anatase at 160 °C/ 1 h, from (a) Ti isopropoxide, (b) Ti oxysulfate, (c) glucose + Ti isopropoxide, (d) glucose + Ti oxysulfate, (e) sucrose + Ti isopropoxide and (f) sucrose + Ti oxysulfate.

Table 2
Characteristics of C-doped titanias synthesized by microwave-hydrothermal reactions using titanium oxysulfate and various C sources at different temperatures for 1 h.

Treatment				Characterization		
Ti source	C source	C:Ti	Temperature (°C)	Crystallite size(nm)		Specific surface area
				XRD	TEM	(m^2/g)
TO$^\delta$	Glucose	3:25	140	8.3	–	–
TO$^\delta$	Glucose	3:25	160	10.9	10–17	158
TO$^\delta$	Glucose	3:25	180	14.3	–	–
TO$^\delta$	Glucose	9:25	140	8.6	–	–
TO$^\delta$	Glucose	9:25	160	10.9	–	–
TO$^\delta$	Glucose	9:25	180	14.4	–	–
TO$^\delta$	Sucrose	3:25	160	11.7	8–12	169
TO$^\delta$	Sucrose	9:25	160	14.5	–	–
TO$^\delta$	Dextrin	3:25	160	10.6	–	163
TO$^\delta$	None	–	160	11.2	8–15	151

TO$^\delta$ = Titanium(IV) oxysulfate.

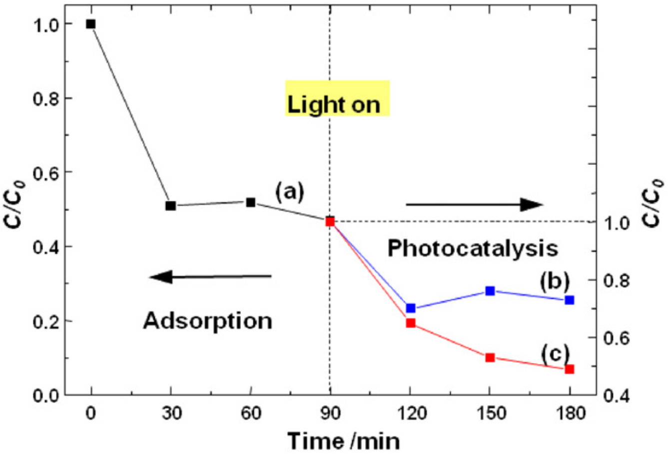

Fig. 3. Methylene blue adsorption and decomposition by C-doped anatase prepared from Ti isopropoxide + glucose at 160 °C/1 h synthesized by microwave-hydrothermal reactions. Adsorption of methylene blue for 90 min without irradiation (a), photocatalytic degradation of methylene blue after MB adsorption for 90 min followed by irradiation with a solar simulator light (b) and an 8 W black light (c).

differences in photocatalytic activities between apparently C-doped and undoped anatase samples.

In terms of the DeNO$_x$ ability of the synthetic samples, the results showed that the photocatalytic activity of carbon-doped titanias, both doped by glucose and sucrose, were higher than those of Degussa P25 commercial sample and undoped or pure titanias (Table 3; Fig. 4), especially under irradiation by long wavelength or visible light (> 500 nm).

Table 3
Crystallite size, BET specific surface area and DeNO$_x$ ability of different samples synthesized by microwave-hydrothermal process.

Sample*	Crystallite size (nm)	S_{BET} (m^2/g)	DeNO$_x$ (%)		
			> 510 nm	> 490 nm	> 290 nm
P25	20.3**	51**	5.4	29	61.2
TI	5.6	235	8.9	35.3	59.7
G-TI	5.3	262	38.8	48.9	69.4
S-TI	5.3	267	41.6	51.2	72.5
D-TI	5.7	236	–	–	–
TO	11.2	151	6.0	14.7	45.1
G-TO	12.5	158	12.0	19.7	63.4
S-TO	11.7	169	20.1	31.3	69.5
D-TO	10.6	163	–	–	–

*P25 = Standard Degussa titania; TI = Ti isopropoxide; TO = Ti oxysulfate; G = glucose; S = Sucrose; D = Dextrin.
**Dong et al. [33].

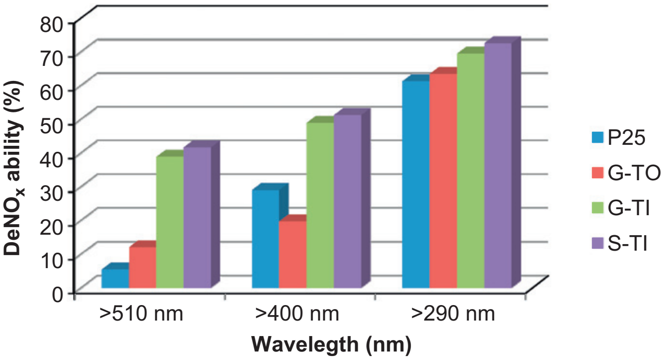

Fig. 4. Bar chart of photocatalytic activities in decomposing NO$_x$ gas at different wavelengths by commerial titania P25 and the samples synthesized by microwave-hydrothermal process (G–TO = glucose + Ti oxysulfate; G–TI = glucose + Ti isopropoxide; S–TI = sucrose + Ti isopropoxide) of this study.

This indicates that the energy band gap is lower in the C-doped titania because of a new energy level formed. When titanias doped with different kinds of carbon sources are compared (Fig. 4), the titania doped by sucrose gave a slightly higher DeNO$_x$ ability than that of glucose because sucrose-doped titanias had higher specific surface areas (Table 3). Titanias with larger specific surface areas can offer more active sites for heterogeneous catalysis and hence the photocatalytic activity in decomposing NO$_x$ was higher with higher surface areas of titanias. A similar explanation is applicable to the two different kinds of titanium sources used in this study. Titanium isopoproxide gave titanias of higher surface are than titanium oxysulfate, and hence titanias from Ti isopropoxide were better for DeNO$_x$ than those made from Ti oxysulfate.

4. Conclusion

Nanoparticles of C-doped and pure or undoped anatase were rapidly synthesized using Ti isopropoxide, Ti ethoxide and Ti oxysulfate with several carbon sources, such as glucose, sucrose or cyclodextrin at 140–180 °C within 1 h. The C-doped anatase materials of very high specific surface area exhibited very high photocatalytic activity in the decomposition of NO$_x$.

Acknowledgments

We would like to thank the Young Scientist and Technologist Program from National Science and Technology Development Agency of Thailand for its financial support.

References

[1] A. Fujishima, K. Honda, Electrochemical photolysis of water at a semiconductor electrode, Nature 238 (1972) 37–38.
[2] G. Pfaff, P. Reynder, Angle-dependent optical effects deriving from submicron structures of films and pigments, Chemical Review 99 (1999) 1963–1981.
[3] L.L. Hench, J.K. West, Sol–gel process, Chemical Review 90 (1990) 33–72.
[4] R.S. Sonawane, S.G. Hegde, M.K. Dongare, Preparation of titanium oxide thin film photocatalyst by sol–gel dip coating, Materials Chemistry and Physics 77 (2002) 744–750.
[5] H.-Y. Lin, C.-Y. Kuo, Photocatalytic activity of TiO$_2$ prepared by microwave/sol–gel method, Reaction Kinetics and Catalysis Letters 98 (2009) 241–247.
[6] R. Leboda, V.M. Gun'ko, M. Marciniak, A.A. Malygin, A.A. Malkin, W. Grzegorczyk, B.J. Trznadel, E.M. Pakhlov, E.F. Voronin, Structure of chemical vapor deposition titania/silica gel, Journal of Colloid and Interface Science 218 (1999) 23–39.
[7] V.M. Gun'ko, V.I. Zarko, V.V. Turov, R. Leboda, E. Chibowski, L. Holysz, E.M. Pakhlov, E.F. Voronin, V.V. Dudnik, Y.I. Gornikov, CVD-Titania on fumed silica substrate, Journal of Colloid and Interface Science 198 (1998) 141–156.
[8] K. Schrijnemakers, N.R.E.N. Impens, E.F. Vansant, Deposition of a titania coating on silica by means of the chemical surface coating, Langmuir 15 (1999) 5807–5813.
[9] A.Y. Stakheev, C.W. Lee, P.J. Chong, Preparatiom and characterization of titanium dioxide embedded onto ZSM-5 Zeolite, Bulletin of the Korean Chemical Society 19 (1998) 530–533.
[10] G. Wu, T. Nishikawa, B. Ohtani, A. Chen, Synthesis and characterization of carbon-doped TiO$_2$ nanostructures with enhanced visible light response, Chemistry of Materials 19 (2007) 4530–4537.
[11] Q. Xiao, L. Ouyang, L. Gao, W. Jiang, One-step hydrothermal preparation and photocatalytic activity of (C, S, Sm)-tridoped

mesoporous TiO_2 photocatalyst under visible light irradiation, Materials Chemistry and Physics 124 (2010) 1210–1215.

[12] C. Lazau, P. Sfirloaga, C. Orha, C. Ratiu, I. Grozescu, Development of a novel fast-hydrothermal method for synthesis of Ag-doped TiO_2 nanocrystals, Materials Letters 65 (2011) 337–339.

[13] S. Komarneni, R. Roy, Q.H. Li, Microwave-hydrothermal synthesis of ceramic powers, Materials Research Bulletin 27 (1992) 1393–1405.

[14] S. Komarneni, R.K. Rajhaa, H. Katsuki, Microwave-hydrothermal processing of titanium dioxide, Materials Chemistry and Physics 61 (1999) 50–54.

[15] S. Yin, B. Liu, T. Sato, Microwave-assisted hydrothermal synthesis of nitrogen-doped titania nanoparticles, Functional Materials Letters 1 (2008) 173–176.

[16] S. Yin, P. Zhang, B. Liu, X. Liu, T. Sato, D. Xue, S.W. Lee, Microwave-assisted hydrothermal synthesis of nitrogen-doped titania photocatalyst and its $DeNO_x$ ability under visible LED light irradiation, Research on Chemical Intermediates 36 (2010) 69–75.

[17] G. Colón, M. Maicu, M.C. Hidalgo, J.A. Navío, Cu-doped TiO_2 systems with improved photocatalytic activity, Applied Catalysis B-Environment 67 (2006) 41–51.

[18] H.S. Park, D.H. Kim, S.J. Kim, K.S. Lee, The photocatalytic activity of 2.5 wt% Cu-doped TiO_2 nano powders synthesized by mechanical alloying, Journal of Alloys and Compounds 415 (2006) 51–55.

[19] M.A. Barakat, H. Schaeffer, G. Hayes, S. Ismat-Shah, Photocatalytic degradation of 2-chlorophenol by Co-doped TiO_2 nanoparticles, Applied Catalysis B- Environment 57 (2005) 23–30.

[20] D. Jing, Y. Zhang, L. Guo, Study on the synthesis of Ni doped mesoporous TiO_2 and its photocatalytic activity for hydrogen evolution in aqueous methanol solution, Chemical Physics Letters 415 (2005) 74–78.

[21] L. Gomathi Devi, B. Narasimha Murthy, Characterization of Mo doped TiO_2 and its enhanced photo catalytic activity under visible light, Catalysis Letters 125 (2008) 320–330.

[22] X. Yang, C. Cao, K. Hohn, L. Erickson, R. Maghirang, D. Hamal, K. Klabunde, Highly visible-light active C- and V-doped TiO_2 for degradation of acetaldehyde, Journal of Catalysis 252 (2007) 296–302.

[23] M.K. Seery, R. George, P. Floris, S.C. Pillai, Silver doped titanium dioxide nanomaterials for enhanced visible light photocatalysis, Journal of Photochemistry and Photobiology A 189 (2007) 258–263.

[24] F. Zhang, Y. Pi, J. Cui, Y. Yang, X. Zhang, N. Gua, Unexpected selective photocatalytic reduction of nitrite to nitrogen on silver-doped titanium dioxide, Journal of Physical Chemistry C 111 (2007) 3376–3756.

[25] Y. Li, M. Ma, W. Chen, L. Li, M. Zen, Preparation of Ag-doped TiO_2 nanoparticles by a miniemulsion method and their photoactivity in visible light illuminations, Materials Chemistry and Physics 129 (2011) 501–505.

[26] M. Zhou, J. Yu, B. Cheng, H. Yu, Preparation and photocatalytic activity of Fe-doped mesoporous titanium dioxide nanocrystalline photocatalysts, Materials Chemistry and Physics 93 (2005) 159–163.

[27] Y. Matsumoto, M. Murakami, T. Shono, T. Hasegawa, T. Fukumura, M. Kawasaki, P. Ahmet, T. Chikyow, S.-y. Koshihara, H. Koinuma, Room-temperature ferromagnetism in transparent transition metal-doped titanium dioxide, Science 291 (2001) 854–856.

[28] E. Borgarello, J. Kiwi, M. Gratzel, E. Pelizzetti, M. Visca, Visible light induced water cleavage in colloidal solutions of chromium-doped titanium dioxide, Journal of the American Chemical Society 104 (1981) 2996–3002.

[29] D. Wu, M. Long, W. Cai, C. Chen, Y. Wu, Low temperature hydrothermal synthesis of N-doped TiO_2 photocatalyst with high visible-light activity, Journal of Alloys and Compounds 502 (2010) 289–294.

[30] S. Hu, A. Wang, X. Li, H. Löwe, Hydrothermal synthesis of well-dispersed ultrafine N-doped TiO_2 nanoparticles with enhanced photocatalytic activity under visible light, Journal of Physics and Chemistry of Solids 71 (2010) 156–162.

[31] W. Sirisaksoontorn, S. Thachepan, A. Songsasen, Photodegradation of phenanthrene by N-doped TiO_2 photocatalyst, Journal of Environmental Science and Health A 44 (2009) 841–846.

[32] Y. Park, W. Kim, H. Park, T. Tachikawa, T. Majima, W. Choi, Carbon-doped TiO_2 photocatalyst synthesized without using an external carbon precursor and the visible light activity, Applied Catalysis B- Environmental 91 (2009) 355–361.

[33] F. Dong, H. Wang, Z. Wu, One-step "Green" synthetic approach for mesoporous C-doped titanium dioxide with efficient visible light photocatalytic activity, Journal of Physical Chemistry A 113 (2009) 16717–16723.

[34] M. Fittipaldi, V. Gombac, T. Montini, P. Fornasiero, M. Graziani, A high-frequency (95 GHz) electron paramagnetic resonance study of B-doped TiO_2 photocatalysts, Inorganica Chimica Acta 361 (2008) 3980–3987.

[35] H. Yu, Photocatalytic abilities of gel-derived P-doped TiO_2, Journal of Physics and Chemistry of Solids 68 (2007) 600–607.

[36] S. Tojo, T. Tachikawa, M. Fujitsuka, T. Majima, Iodine-doped TiO_2 photocatalysts correlation between band structure and mechanism, Journal of Physical Chemistry C 112 (2008) 14948–14954.

[37] D. Li, H. Haneda, S. Hishita, N. Ohashi, N.K. Labhsetwar, Fluorine-doped TiO_2 powders prepared by spray pyrolysis and their improved photocatalytic activity for decomposition of gas-phase acetaldehyde, Journal of Fluorine Chemistry 126 (2005) 69–77.

[38] R. Asahi, T. Morikawa, T. Ohwaki, K. Aoki, Y. Taga, Visible-light photocatalysis in nitrogen-doped titanium oxides, Science 293 (2001) 269–271.

[39] H. Irie, Y. Watanabe, K. Hashimoto, Nitrogen-concentration dependence on photocatalytic activity of $TiO_{2-x}N_x$ powders, Journal of Physical Chemistry B 107 (2003) 5483–5486.

[40] T. Ihara, M. Miyoshi, Y. Iriyama, O. Matsumoto, S. Sugihara, Visible-light-active titanium oxide photocatalyst realized by an oxygen-deficient structure and by nitrogen doping, Applied Catalysis B-Environmental 42 (2003) 403–409.

[41] A. Zaleska, Doped TiO_2: a review, Recent Patents on Engineering 2 (2008) 157–164.

[42] S. Sakthivel, H. Kisch, Daylight photocatalysis by carbon-modified titanium dioxide, Angewandte Chemie International Edition 42 (2003) 4908–4911.

[43] H. Li, D. Wang, H. Fan, P. Wang, T. Jiang, T. Xie, Synthesis of highly efficient C-doped TiO_2 photocatalyst and its photo-generated charge-transfer properties, Journal of Colloid and Interface Science 354 (2011) 175–180.

[44] S. Lee, C.Y. Yun, M.S. Hahn, J. Lee, J. Yi, Synthesis and characterization of carbon-doped titania as a visible-light-sensitive photocatalyst, Korean Journal of Chemical Engineering 25 (2008) 892–896.

[45] S. Komarneni, V.C. Menon, Q.H. Li, R. Roy, F. Ainger, Microwave-hydrothermal Processing of $BiFeO_3$ and $CsAl_2PO_6$, Journal of the American Ceramic Society 79 (1996) 1409–1412.

[46] A. Kremenovic, B. Antic, J. Blanusa, M. Comor, P. Colomban, L. Mazerolles, E.S. Bozin, Heterogeneity and disorder in $Ti_{1-x}Fe_yO_{2-d}$ nanocrystal rutile-based flowerlike aggregates: detection of anatase, Journal of Physical Chemistry C 115 (2011) 4395–4403.